Estimation of Projector Defocus Blur by Extracting Texture Rich Region in Projection Image

Yuji Oyamada and Hideo Saito
Graduate School of Science and Technology, Keio University
3-14-1 Hiyoshi Kohoku-ku
223-8522, Yokohama, Japan

{charmie, saito}@ozawa.ics.keio.ac.jp

ABSTRACT

To use a projector anytime anywhere, a lot of projector-camera based approaches have been proposed. Focal correction technique, one of them, reduces the effect of defocus blur which occurs when a screen is located out of projector's depth-of-field. To achieve focal correction, we have to estimate the degree of defocus blur on the displayed images. Some previous methods use any special pattern images. A method which needs no special image has been proposed, however, this method can't estimate at less-textured or already blurred region in the projection image. In this paper, we propose a novel method for estimating PSF (Point Spread Function) without projecting any special pattern images. To prevent such an estimation error, we search and extract well-suited regions to estimate PSF in the projection image and estimate the PSF at extracted region. Experimental results show that our method can prevent PSF estimation error without any special images.

Keywords

Projector-Camera System, defocus blur estimation, projector defocus, pre-correction, image enhancement

1. INTRODUCTION

Projectors have been improved in their quality. The improvement in their capabilities (e.g. brightness, resolution, contrast and throw-distance) has made projectors one of the popular display devices. The greatest merit of a projector is that a projector can project onto many screens of various sizes and scaled-up projection can show displayed image to many observers. So a lot of projector based application have been proposed [Cra05, Gup06, Muk07, Ras01, Yot02]. Recently, a lot of projector-camera based approaches that aim to allow projector to project onto complex everyday surfaces have been proposed. These methods correct the projection image to display the image as a projector projects onto a planar white screen from perpendicular position to the screen.

There projector-camera based correction techniques are mainly categorized into three types. Geometric warping, correcting geometric distortion, allows projector to project onto a non-planar screen and aligns multiple projectors projection. Radiometric compensation, corrects color variation caused by color of a screen object or environmental lighting, allow projector to project a colored and textured screen under strong environmental lighting. Focal correction, reduces the effect of defocus blur, makes projector's depth-of-field wider.

In general, these methods use any measuring images (e.g. chess board and uniform colored image) to know a relation about focus between a projection image and a displayed image. In previously focal correction techniques, fiducial images which has white rectangle array on a black background have been used to estimate focal relation [Bim06, Bro06, Zha06]. Furthermore, we have proposed a novel method which requires no fiducial images to estimate this focal relation [Oya07]. The reason why we don't use any special measuring image is that projecting and displaying any measuring images interrupts an effect of projector based application. However, estimation error can occur by our previous method. When the projection image is less-textured or has not in-focus region, the estimated PSF parameter is not accurate. Because such an image is insusceptible to the projection defocus blur.

In this paper, we propose a novel method for estimating focal relation between a projection image and a displayed image without projecting any measuring images. To estimate focal relation accurately, we extract well-suited regions for PSF parameter estimation and estimate the PSFs at extracted regions. Experimental results show that our method can estimate the PSF more accurate than our previous method, in which fixed region and sub-image is used for PSF estimation.

2. RELATED WORK
2.1. Geometric Warping
Geometric warping technique has been developed. To display an undistorted image at one projector system, the system needs to know projector-camera mapping. When a screen is planar, we can represent this projector-camera mapping as a homography [Che02]. To apply a screen with complex surface, the projector-camera mapping requires at the pixel level [Tar03]. To align multiple projections, the system needs projector-projector mapping as well as each projector-camera mapping [Ras99, Ras04, Tar03].

2.2. Radiometric Compensation
To project onto colored or textured screen with strong environmental light, radiometric compensation techniques have been proposed. Color mapping between projector and camera can be obtained by projecting a lot of uniform color images. Compensation techniques for both static [Nay03, Gro04] and dynamic scene [Fuj05] have been proposed. Ashdown et al. have proposed content-dependent compensation technique that based on both radiometric model and human visual system [Ash06]. Wetzstein et al. have proposed compensation method that accounts for all possible local and global illumination effects by applying the inverse light transport between a light source and a projector which describes all illumination [Wet06].

2.3. Focal Correction
To extend projector's depth-of-field, there are mainly two solutions in projector-camera based approaches. Bimber et al. projected images projected by multiple projectors with adjusted different focal planes to minimize infection of defocus blur [Bim06]. Another projected an image pre-corrected to cancel out defocus blur [Bro06, Oya07, Zha06]. To achieve both methods, estimating PSF which represent how much degree displayed image is blurred is important. To estimate PSF, the fiducial image is frequently used because it acts as an impulse function. Rasterizing the feature images estimates a series of PSF at every pixel in the displayed image. Assuming

object screen planar, Brown et al. estimate focal relation from a fiducial image projection [Bro06]. We estimate focal relation from projection result of projected image which an observer really wants [Oya07]. For real application, displaying any fiducial images is unwanted. In that sense, unused fiducial image method is better. However, estimation error can occur, when the divided region in the projection image is less-textured or has not in-focus region, the estimated focal relation is not accurate.

In this paper, we propose a novel method for estimating PSFs on a planar screen without projecting any special pattern images. To estimate PSF accurately, we extract sub-region which is well-suited for PSF estimation in the projection image and estimate PSFs at each extracted region. Experimental results show that our method can prevent the PSF estimation error without any special image projection.

3. PROPOSED METHOD
Our system is consists of a projector, a camera and a planar screen as shown in Fig. 1(a). However, there are a variety of image defection factors that deteriorate a displayed image on the screen. For example, when we project an original image (as shown in Fig. 1(b)), displayed image is geometric and radiometric distorted and defocus blurred as shown in Fig. 1(c). To estimate the degree of defocus blur accurate, we have to remove image defection factors, geometrical and radiometric distortion, other than projection defocus blur. To remove them, we use a calibrated projector-camera. When we project a projection image (as shown in Fig. 1(d)) which is warped and compensated based on homography and Color Transfer Function, the displayed image is deteriorated by only a defocus blur as shown in Fig. 1(e). As same as generating the projection image, we predict an image which is a projection result of the projection image.

The proposed method first extracts regions are well-suited to PSF parameter estimation and then estimate PSF by comparing the displayed image with the predicted image at every extracted region. Finally, we project the pre-corrected image (as shown in Fig. 1(f)) corrected based on the estimated PSFs. The displayed pre-corrected image can reduce the effect of projector defocus blur as shown in Fig. 1(g).

3.1. Image Blurring and Deblurring
The projection defocus blur can be represented by the 2D Gaussian type PSF $h(x, y)$ with the sigma σ as Eq. (1)

(a) System configuration

(b) Original image   (c) Displayed (b)

(d) Projection image   (e) Displayed (d)
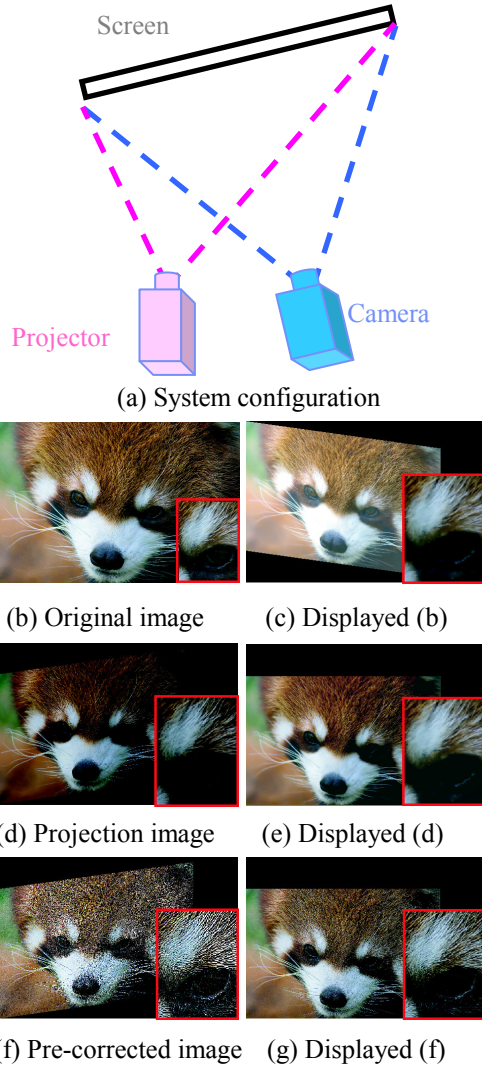
(f) Pre-corrected image   (g) Displayed (f)

Figure1: Relationship between camera image and projector image

(Left column) projector images

(Right column) camera images

$$h(x,y) = \frac{1}{2\pi\sigma^2} \exp\left(-\frac{x^2+y^2}{2\sigma^2}\right) \quad (1)$$

A blurred image $g(x,y)$ can be represented with a convolution of PSF $h(x,y)$ on the original image $f(x,y)$ as shown in Eq. (2).

$$g(x,y) = f(x,y)*h(x,y) \quad (2)$$

Based on the traditional image processing technology, we can restore the unknown original image by convolution with an inverse function $h(x,y)^{-1}$ on the blurred image. The main topic of traditional image restoring is how to estimate the PSF and how to restore the unknown original image using estimated PSF. In the case of defocus projection blur, we know

the type of PSF and an original image that we would like to display on a target screen. Therefore, we can display the original image by projecting a pre-corrected image $\widetilde{f}(x,y)$, in which the defocus blur is previously deblurred.

$$\begin{aligned} f(x,y) &\approx \widetilde{f}(x,y)*h(x,y) \\ &= \left[f(x,y)*h^{-1}(x,y)\right]*h^{-1}(x,y) \end{aligned} \quad (3)$$

We can represent convolution in the spatial domain as the product in the frequency domain, where the blurring is represented as

$$G(u,v) = F(u,v)H(u,v) \quad (4)$$

where G, F and H are Fourier transforms of g, f and h respectively. If we know the PSF, we can apply Wiener Filtering, which is one of the popular solutions that minimize the effect of noise. The Wiener Filter H_w is given as

$$H_W = \frac{1}{H}\frac{|H|^2}{|H|^2+\gamma} \quad (5)$$

where γ is the signal-to-noise ratio in power.

3.2. Projection Image Generation

To remove image defection factors, geometrical distortion and color variation, other than projection defocus, we generate a new projection image and predict a projection result of the projection image. We refer to an image projected by the projector as the *projection image*, a displayed image on the screen captured by the camera as the *displayed image* and a prediction of the displayed image as the *predicted image*.

3.2.1. Geometric Calibration

To correct geometric distortion, we need to know mapping between camera pixel and projector pixel. In the case of a planar screen, we can model this mapping as a 3x3 planar perspective transformation matrix homography [Che02]. This allows us to generate a projection image from non-distorted image on the screen. Projecting this generated projection image, we can display as if projector is located at perpendicular position to the screen.

In proposed method, we project 24 fiducial images which have a white rectangle on the black background on a target screen. Then, we calculate a homography between a projection image and a displayed image by comparing these images. Using calculated homography, we make a new projection image to display as the displayed image is not geometrically distorted.

3.2.2. Radiometric Calibration

To correct radiometric color variation, we need to know color mapping between camera and projector. This color mapping can be described as a Color Transfer Function *CTF* [Jay04]. A pixel value in the projected image $I_p(x, y)$ is changed to a pixel value in the captured image $I_c(x, y)$ by using calculated CTF $C(I)$

$$
\begin{aligned}
I_c(x, y) &= C(I_c(x, y)) \\
&= \frac{a}{1 + e^{-\alpha(C(I_p(x,y) - b))}} + k
\end{aligned} \quad (6)
$$

where a, b, k and α are parameter. Fig.3 (a) describes color reference between projected color values and displayed one. In proposed method, we project 17 uniform color images. Then, we calculate a Color Transfer Function between a projection color projected by the projector and a displayed color captured by a camera by comparing these images. In Fig. 2(a), blue points represent captured color value
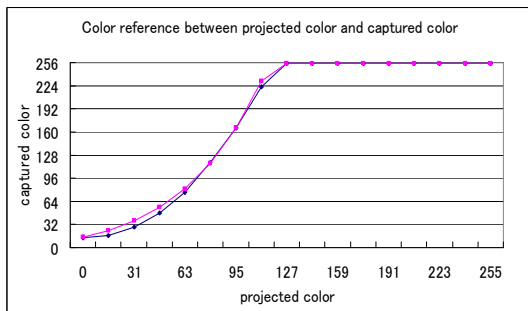
(a) Color reference between projected color and captured color
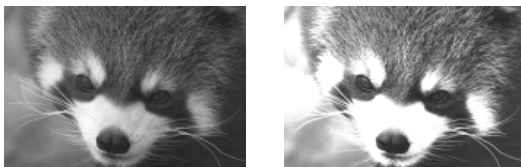
(b) Original image   (d) Displayed (b)
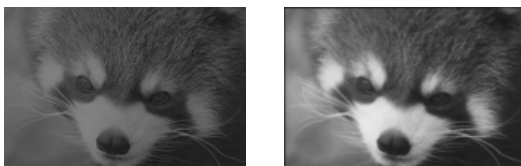
(c) Compensated (b)   (e) Displayed (c)

Figure2: Results of radiometric compensation

(Top row) color reference graph between projected color value and displayed color value

(Left column) projector images

(Right column) camera images

and pink points represent calculated color value using CTF.

Fig. 2(b)-(e) are examples which explain how CTF works. As shown in Fig. 2(d), a projection result of original image Fig. 2(b) is different from the original image in color. Fig. 2(c) is result of radiometric compensation using calculated CTF. Comparing Fig. 2(e), a projection result of the compensated image, with the original image, the result of compensated image is closer to the original image than other images.

3.2.3. Displayed Image Prediction

Applying these two calibrations, here are two mappings between a camera image and a projector image, homography and CTF. In this section, we explain how to create a projection image for displaying as we project onto white planar screen from perpendicular position and predict a displayed image on the screen.

First, we scaled down or up an original image to fit the image to the projection range. Then, we compensate the scaled image using calculated CTF. Finally, we warped the compensated image using calculated homography. This warped image is a projection image to display the image on the screen which we want to display. By the reverse method, we predict the image which would display on the screen by projection from the projection image using homography and CTF.

3.3. PSF Estimation Regions Extraction

Our target screen is planar, so the types of the defocus blur are categorized into two types. When the projection is on-axis, the degree of defocus blur is homogenous throughout the displayed image. On the other hand, in the case of the off-axis projection, the degree of defocus blur is non-homogenous. To handle both cases, we have to estimate the PSF on a pixel by pixel. Based on a defocus blur characteristic that the degree of defocus blur is proportional to the distance between the screen and the focal length, we calculate pixel by pixel PSFs from at least four PSFs by linear interpolation. The simplest extraction these four regions for interpolation uses four corner regions of the image. However, corner of a picture is not useful region to estimate PSF, because a camera usually focus on a photographic subject which is located at center of the picture, so surrounding region can be not in-focus region. To estimate the PSFs on a displayed image more accurate than previous method, we extract four divided regions suited to PSF estimation. First of all, we define what well-suited and unsuited region for PSF estimation is. Basic idea for the definition come from the method creates an
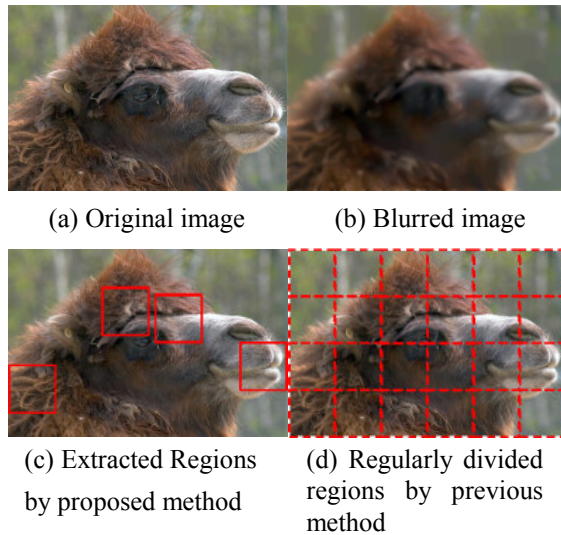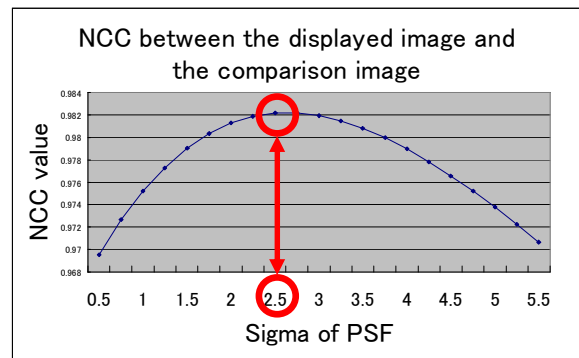
(a) Original image　　(b) Blurred image

(c) Extracted Regions by proposed method

(d) Regularly divided regions by previous method

Figure3: Rich textured region extraction

(a) NCC graph

(b) Predicted image　　(c) Displayed image

(d) Comparison images

Figure4: PSF estimation

NCC graph between the displayed image (c) and the comparison images (d) result of convolution different PSFs on the original image (b)
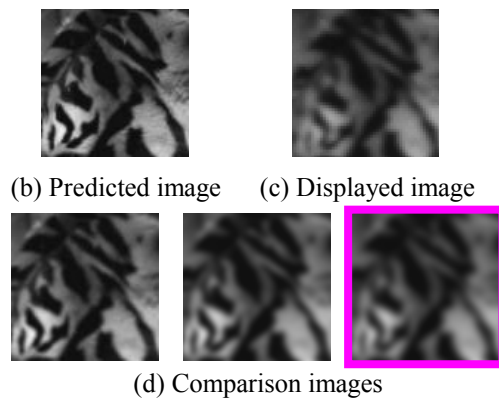
arbitrary focused image proposed by Aizawa et al. [Aiz00]. When a projection image is less textured or already blurred, estimation error happens. So we define the region affected by much defocus blur as well-suited region for PSF estimation. To extract well-suited region, we compare an original image (as shown in Fig. 3(a)) with a blurred image (as shown in Fig. 3(b)) which is result of convolution of PSF on the original image. First, we calculate SSD(Sum of Squared Difference) between the original image and the blurred image. The sub-image with the highest SSD value is the most infected regions. We define this region as well-suited region for PSF estimation (red framed region in Fig. 3(c)). By comparing the extracted regions with regularly divided regions (dashed red framed region in Fig. 3(d)), we can confirm that the extracted region is textured and in-focus region. On the other hand, there are some not in-focus regions in the regularly divided regions.

3.4. PSF Parameter Estimation

As mentioned in previous section, to estimate non-uniform PSFs on a planar screen, we interpolate the each PSF from four PSFs at extracted well textured regions (as mentioned in Sec. 3.1.). To estimate PSF on the extracted region, we generate multiple comparison images (as shown in Fig. 4(d)) by convolution different PSFs on the predicted image (Fig. 4(b)). Next, we calculate NCCs(Normalized Cross Correlation) between each comparison image and the displayed image. The PSF of the comparison image with the highest correlation to the displayed image is the PSF which represents the defocus blur on the extracted region in the displayed image. Fig. 4 is an example of this PSF parameter estimation. In this case, NCC graph as shown in Fig. 4(a) indicates

that the comparison image which sigma value is 2.5 (right image of Fig. 4(d)) has highest correlation to the displayed image (as shown in Fig. 4(c)). By applying this estimation at every extracted region, here are four piecewise-constant PSFs corresponding to extracted regions with rich texture. We calculate every PSF at each pixel from these four PSFs.

4. EXPERIMENTAL RESULT

The proposed method has been tested about suited regions extraction and PSF parameter estimation. As shown in Fig. 5, projection images are projected by a projector (EPSON ELP7600) which is in front of a target screen. Displayed images on the screen are captured by a camera (SONY XCDC710CR). The projection image is 960x640 pixels resolution and extracted region is 160x160 pixels resolution.

4.1. Suited Regions Extraction

First, we examine suited regions extraction method. Original images consist of foreground region
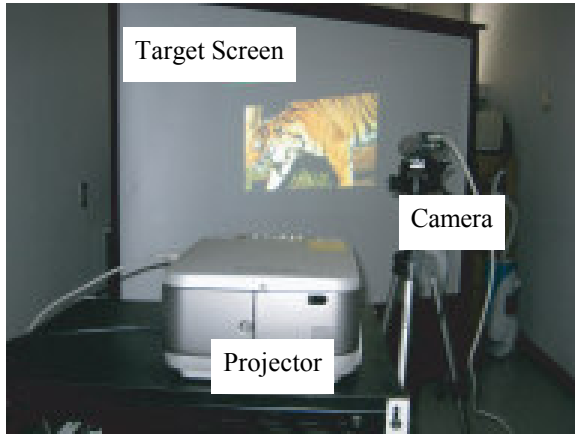
Figure5: Experimental environment

(an animal) and background region have both in-focus region and not in-focus region. In the "tiger" image, bottom right and bottom left corners are not in-focus as shown in Fig. 6(h) and (i). In the "dog" image, top left and right top regions are not in-focus, especially the background of the top left except the dog ear. The expected results of suited regions extraction are that extracted regions are located on
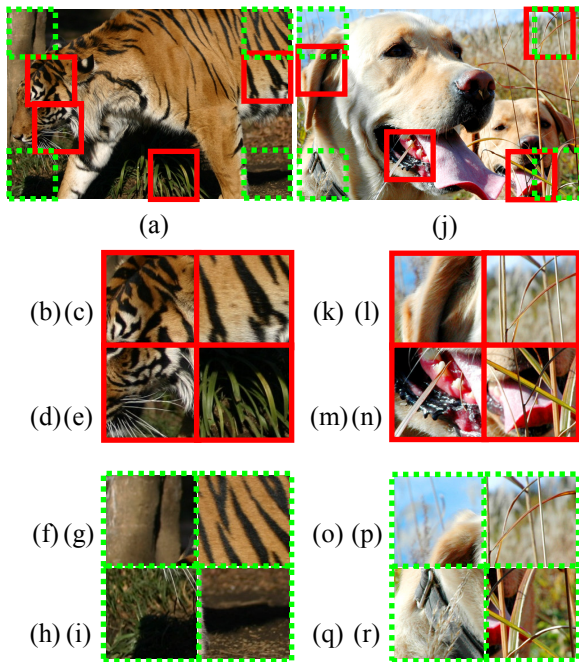

Figure6: Result of suited regions extraction
(Top row): Extracted regions (red marked) and image corners (green dashed line)
(Middle row): Zoomed extracted regions (red line)

(Bottom row): Zoomed four corners of the original image (green dashed line)

foreground region (animal). Fig. 6 shows the result of proposed suited regions extraction method. Red marked regions in Fig. 6(a) correspond to the extracted results. Both middle and bottom row are zoomed regions, respectively extracted regions (as shown in Fig. 6(b)-(e) and (k)-(n)) and image corners (as shown in Fig. 6(f)-(i) and (o)-(r)). Comparing extracted regions with four corners of the image, extracted regions are well-textured and in-focus regions. Extracted right bottom corner on the "tiger" image and right top corner on the "dog" image are not exactly foreground regions. However, these regions are well-textured and in-focus, so these regions are well suited for PSF parameter estimation more than other region in foreground. On the other hand, some image corners Fig. 6(h), (i) and (o) are less-textured and not in-focus regions. These results show that proposed suited regions extraction works well.

4.2. PSF Parameter Estimation

Next, we tested the accuracy of PSF parameter estimation method at both perpendicular and slanted projection case using these two images which have both in-focus region and not in-focus region. We use a fiducial image which is used by the previous methods [Bim06, Bro06, Zha06] and consider that the PSF parameter estimated by using the fiducial image is correct parameter. In this experiment, we compare the PSF parameter estimated by using both projection image and the fiducial image at both extracted regions and image corners.

4.2.1. Perpendicular Projection

First, we locate a screen in the perpendicular direction to a projector out of the projector's depth-of-field. In this situation, projector defocus blur can be uniform, so expected result is that estimated PSF parameters are same. Fig. 7 shows the result of the perpendicular projection defocus. Left column of Fig. 7 corresponds to the result of the "tiger" image and right is the "dog" image's one. Top row is displayed image, middle row is estimated PSF parameter at extracted region and bottom row is estimated PSF parameter at image corner. In this situation, the PSF parameters estimated by using the fiducial image at image corners Fig. 7(o)-(r) and at extracted regions are correct parameters. By comparing the PSF parameters estimated by using the projection image (Fig. 7(b)-(e) and (f)-(i)), we can see that the every parameter estimated at extracted regions is absolutely equal. On the other hand, the PSF parameter estimated at image corner (Fig. 7(f)-(i)) shows that the estimation error is observed at right bottom corner (Fig. 7(i)). Because the right bottom corner of the projection image is not in-focus region, so this estimation error occurs. This result means that we can estimate PSF parameter accurately at the extracted region more than the image corner.

(a)   (j)

(b) (c)   [3.5 | 3.7]   (k) (l)   [3.5 | 3.7]

(d) (e)   [3.5 | 3.5]   (m)(n)   [3.5 | 3.5]

(f) (g)   [3.2 | 4.0]   (o) (p)   [3.7 | 3.7]

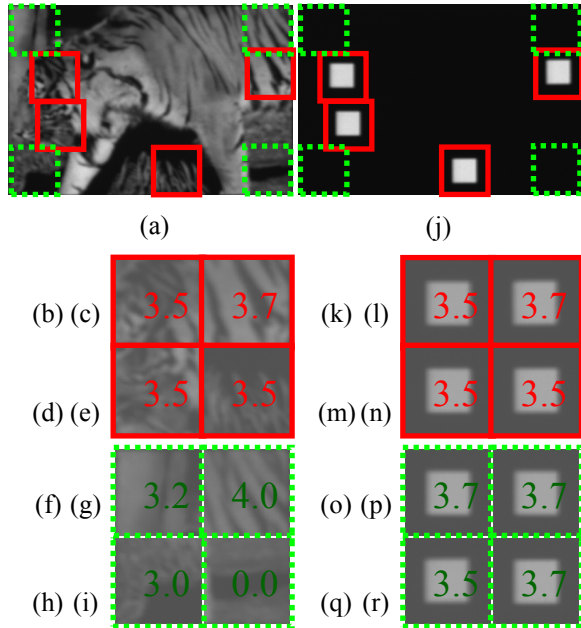(h) (i)   [3.0 | 0.0]   (q) (r)   [3.5 | 3.7]

Figure7: Result of PSF parameter estimation at perpendicular projection

(Top row): displayed images

(Middle row): Estimated PSF parameter at extracted region (red line)

(Bottom row): Estimated PSF parameter at image corner (green dashed line)

4.2.2. Slanted Projection

Next, we locate the screen in the slanted direction to the projector. In this case, left side of the displayed image is in-focus and right side is blurred. Fig. 8 shows the result of slanted projection defocus and each row and column is as same as Fig. 7. Fig. 8(k)-(n) and (o)-(r) are respectively corresponding to the PSF parameters estimated by using the fidicial image at the extracted regions and the image corners. By comparing the PSF parameters estimated by proposed method (Fig. 8(b)-(e)) with these estimated parameters, every parameter is estimated lower but gradually increases from left to top. On the other hand, seeing estimated parameter by using the projection image at image corner (Fig. 8(f)-(i)) shows that every estimated PSF parameter is zero and is evidently incorrect. Because the every image corner of this projection image "dog" is not in-focus, so the estimated parameters are insusceptible to the projection defocus blur.

5. CONCLUSION

In this paper, we propose a novel method for estimating PSF on a planar screen without projecting any special pattern images. By assuming richly

(a)   (j)

(b) (c)   [0.0 | 1.0]   (k) (l)   [0.0 | 1.0]

(d) (e)   [1.0 | 1.2]   (m)(n)   [1.0 | 1.2]

(f) (g)   [0.0 | 0.0]   (o) (p)   [0.0 | 2.0]

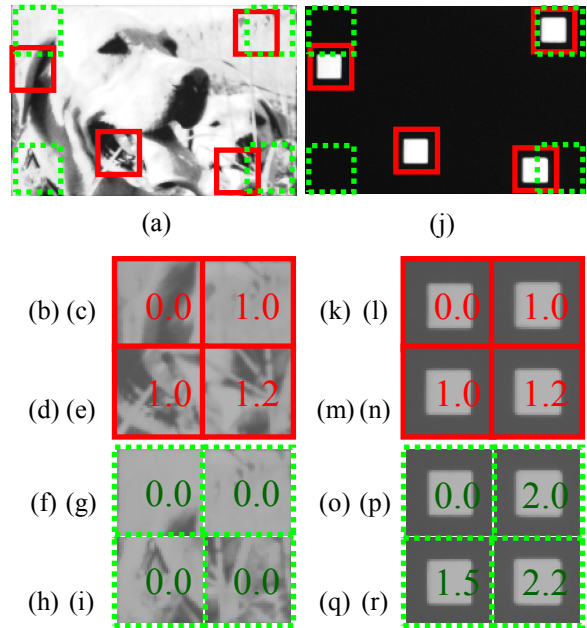(h) (i)   [0.0 | 0.0]   (q) (r)   [1.5 | 2.2]

Figure8: Result of PSF parameter estimation at slanted projection

(Top row): displayed images

(Middle row): Estimated PSF parameter at extracted region (red line)

(Bottom row): Estimated PSF parameter at image corner (green dashed line)

textured and in-focus region as a well-suited region for PSF estimation, we can extract the region suited to PSF estimation. Experimental results show that our method can estimate the PSF parameter on the displayed image, even the projection image has some regions which are less-textured and not in-focus.

6. ACKNOWLEDGEMENTS

7. REFERENCES

[Aiz00] Aizawa, K., Kodama, K., Kubota, A Producing object-based special effects by fusing multiple differently focused images: IEEE Transactions on Circuits and System for Video Technology, pp.323-330, 2000

[Ash06] Ashdown, M., Okabe, T., Sato, I. and Sato, Y. Robust Content-Dependent Photometric Projector Compensation: proceedings of the CVPR'06, pp.6, 2006

[Bim06] Bimber, O. and Emmerling, A. Multifocal Projection: A Multiprojector Technique for Increasing Focal Depth: IEEE Transactions on Visualization and Computer Graphics, Vol.12, pp.658-667, 2006

[Bro06] Brown, M. S., Song, P. and Cham, T. J. Image Pre-Conditioning for Out-of-Focus Projector Blur: proceedings of the CVPR'06, pp.1956-1963, 2006

[Che02] Chen, H., Sukthankar, R., Wallace, G. and Li, L. Scalable alignment of large-format multi-projector displays using camera homography trees: proceedings of VIS'02, pp.339-346, 2002.

[Cra05] Crasto, D., Kale, A. and Jaynes, C. The Smart Bookshelf: A study of camera projector scene augmentation of an everyday environment: workshop on Applications of Computer Vision, pp.218-225, 2005

[Fuj05] Fujii, K. Grossberg, M. D. and Nayar, S. K. A Projector-Camera System with Real-Time Photometric Adaptation for Dynamic Environments: proceedings of CVPR'05, pp.814-821, 2005

[Gro04] Grossberg, M. D., , Peri, H. Nayar, S. K. and Belhumeur P. N. Making One Object Look Like Another: Controlling Appearance Using a Projector-Camera System: journal of CVPR, Vol.1, pp.452-459, 2004

[Gup06] Gupta, S. and Jaynes, C. The Universal Media Book: Tracking and Augmenting Moving Surfaces With Projected Information: proceedings of the ISMAR'06, pp.177-180, 2006

[Jay04] Jaynes, C., Webb, S. and Steele, R. M. Camera-Based Detection and Removal of Shadows from Interactive Multiprojector Displays: IEEE Transactions on Visualization and Computer Graphics. Vol.10, pp.290-301, 2004

[Muk07] Mukaigawa, Y., Sumino, K. and Yagi, Y., High-Speed Measurement of BRDF usingan Ellipsoidal Mirror and a Projector: workshop on PROCAMS'07

[Nay03] Nayar, S. K., Peri, H., Grossberg, M.D. and Belhumeur, P. N. A Projection System with Radiometric Compensation for Screen Imperfections: workshop on PROCAMS2003, 2003

[Oya07] Oyamada, Y. and Saito, H. Focal Pre-Correction of Projected Image for Deblurring Screen Image: workshop on PROCAMS'07, 2007

[Ras99] Raskar, R., Brown, M. S., Yang, R., Chen, W. C. Welch, G. Towles, H. Seales, B. and Fuchs, H. Multi-projector displays using camera-based registration: proceedings of VIS'99, pp.161-168, 1999.

[Ras01] Raskar, R., Welch, G., Low, K. L. and Bandyopadhyay, D. Shader Lamps: Animating Real Objects With Image-Based Illumination: proceedings of the 12th Eurographics Workshop on Rendering Techniques, pp.89-102, 2001

[Ras04] Raskar, R., Baar, J. V., Willwacher, T. and Rao, S. Quadric Transfer for Immersive Curved Screen Displays: journal of Computer Graphics Forum, Vol.23, pp.451-460, 2004

[Sen05] Sen, P., Chen, B., Garg, G., Marschner, S. R., Horowitz, M., Levoy, M. and Lensch H. P. A. Dual photography: ACM Transactions on Graphics, Vol.24, pp.745-755, 2005

[Tar03] Tardif, J. P., Roy, S. and Trudeau, M. Multi-projectors for arbitrary surfaces without explicit calibration nor reconstruction: proceedings of 3DIM2003, pp.217-219, 2003

[Wet06] Wetzstein, G. and Bimber, O. Radiometric compensation of global illumination effects with projector-camera systems: proceedings of SIGGRAPH'06, pp.38, 2006

[Yot02] Yotsukura, T., Nielsen, F., Binsted, K., Morishima, S. and Pinhanez, C. S. Hypermask: Talking Head Projected onto Real Object: journal of The Visual Computer, pp.111-120, 2002

[Zha06] Zhang, L. and Nayar, S. K. Projection defocus analysis for scene capture and image display: proceedings of SIGGRAPH'06, pp.907-915, 20